A localized 2010 in situ burning operation in the Gulf of Mexico created a large smoke plume. *Reprinted from Gullett et al. (2016), Graphical Abstract, with permission from Elsevier.*

WHAT WAS RELEASED?

Assessing the Physical Properties and Chemical Composition of Petroleum and Products of Burned Oil

By Jürgen Rullkötter and John W. Farrington

ABSTRACT. The severity of oil spills depends on the quantity of material released and its physical and chemical properties. The total amount of petroleum spilled during the Deepwater Horizon incident and the relative fractions of the chemical compound classes of the Macondo oil were obtained by measurements, observations, and model calculations, with a significant amount of uncertainty. Because petroleum is an extremely complex mixture of many thousands or more of gaseous, liquid, and solid constituents, full elucidation of their compositions at the molecular level is impossible with presently available analytical techniques. This paper reviews published work on widely used analytical techniques and points out that scientists' varying approaches to research questions and preferences for methods of analysis constitute a source of uncertainty. In addition, the focus is on two technical advancements developed over the last two decades, namely two-dimensional gas chromatography and Fourier transform ion cyclotron resonance mass spectrometry. Both were particularly valuable in the analysis of the spilled Macondo oil and its weathering products. Among the different processes of alteration of the original oil, only in situ oil burning is dealt with in this paper. This review reveals the paucity of data on this mitigation process and shows the need for more systematic coordination of methods in burned oil research studies.

INTRODUCTION

The significance of the Deepwater Horizon (DWH) oil spill arises from the sheer quantity of petroleum released, uncontrolled, from the Macondo petroleum reservoir—it is the largest incident of this kind in history. Addressing the full impact of the released petroleum on Gulf of Mexico flora and fauna, coastal areas, and human health requires consideration of both the quantity and the chemical composition of discharged materials.

This paper addresses estimated quantities of original petroleum discharged from the damaged DWH wellhead at the bottom of the Gulf of Mexico as well as the physical properties and chemical composition of the petroleum released into the environment. The complexity of petroleum, in itself, poses a barrier to conducting an analysis that everyone can agree upon. Investigators use their varying preferred methods, with attendant additional problems and uncertainties.

The products that result from the burning of oil as a specific measure in oil spill response are a second aspect of this review; other papers in this special issue examine the use of dispersants (Quigg et al., 2021) and alteration of the original petroleum by physical (e.g., evaporation, dissolution), chemical (e.g., photo-oxidation by sunlight at the water surface), and biological processes (microbial transformation and degradation), collectively called weathering (Farrington et al., 2021).

PETROLEUM

Petroleum is generated from the remnants of (mainly) plant biomass in fine-grained sediments deposited long ago in aquatic environments under low oxygen conditions. Upon progressive burial, the sediments are compacted into petroleum source rocks, typically at depths of several thousand meters. Over millions of years, the organic material in these rocks is transformed into gas and oil under the influence of geothermal heat flow. Increase in pressure due to the conversion of solid material into gases and liquids forces these products out of the source rocks into more porous carrier rocks. The petroleum then migrates upward because its density is lower than that of pore waters. When it reaches a rock formation that is isolated at the top by an impermeable cap rock (like claystone or salt), it accumulates in a deep reservoir rock (e.g., Tissot and Welte, 1984; Hunt, 1996; Welte et al., 1997; Overton et al., 2016).

Petroleum is an extremely complex mixture of many thousands, if not millions, of individual constituents at the molecular level. As used by the oil industry, petroleum is a collective term comprising gaseous (natural gas), liquid (crude oil), and solid (asphalt) components. Due to co-dissolution effects and elevated temperatures, petroleum commonly exists as a single phase or in two phases (gas and liquid) in reservoirs.

Physical Properties

The most common physical properties used to describe petroleum are density, viscosity, and boiling point ranges. The density of crude oils is usually expressed as API (American Petroleum Institute) gravity, which is inversely related to specific density. Viscosity, a measure of a fluid's internal resistance to flow at a given temperature and pressure, depends on the chemical composition of the petroleum, including the amount of dissolved gas it contains. The upstream oil industry (i.e., refineries) uses the boiling point properties of crude oils to produce distillation fractions (cuts) of defined boiling ranges, each with a mixture of different chemical compound types. These cuts, after further refinement, are the oil fractions known as gasoline, kerosenes (jet fuels), fuel oils, and others.

A broad classification of petroleum is that of light or heavy oil, based upon viscosity or API gravity (Table 1). According to this scheme, the Macondo oil of 40° API gravity spilled in the Gulf of Mexico in 2010 is a light oil lean in sulfur content (<0.5% wt.; "sweet"; Reddy et al., 2012).

Chemical Composition – General Aspects

Analysis of spilled oil in terms of its origin and transformation by physical (evaporation, dissolution) or (bio)chemical (photo-oxidation, microbial oxidation, selected incorporation into biomass or other forms of metabolism) processes is in most cases targeted toward its chemical composition rather than its physical properties. The common strategy applied as a first step, after evaporation of the most volatile components (topping), is to separate the complex mixture of oil components into compound classes by polarity using liquid chromatography with various adsorbents on thin-layer plates, in gravity columns, or by medium-pressure or high-performance liquid chromatography. The compound classes usually obtained are saturated hydrocarbons (alkanes), aromatic hydrocarbons (including some heteroaromatic species), resins, and asphaltenes (SARA). Saturates, aromatics, and resins com-

TABLE 1. Oil classification by API gravity ranges with a few examples from different sources. For comparison, water has an API gravity of 10°.

OIL TYPE	API GRAVITY*	EXAMPLES (API)	REFERENCES
Condensate	>45°	Agbami, Nigeria (48°)	Speight (2015)
Light oil	35°–45°	West Texas Intermediate (40°), Macondo (40°)	Speight (2015) Reddy et al. (2012)
Medium oil	25°–35°	Alaska North Slope (32°)	Speight (2015)
Heavy oil	15°–25°	Venezuela Heavy (17°)	Speight (2015)
Extra heavy oil	<15°	Tar sands: Orinoco, Venezuela (8°–12°), Athabasca, Canada (6°–10°)	Tissot and Welte (1984)

* API gravity = (141.5/specific gravity at 15.6°C) – 131.5

prise a single solubility fraction, collectively called "maltenes." They are soluble in alkane solvents (most commonly *n*-pentane or *n*-heptane), while the asphaltenes are isolated by alkane solvent precipitation (insolubility). Further subfractions can be obtained by employing a number of more sophisticated techniques (e.g., Peters et al., 2005a).

Alkane (Figure 1) is a synonym for a saturated hydrocarbon (i.e., a chemical compound that contains only carbon and hydrogen and has no double bonds or aromatic units). Alkanes can be straight chains of CH_2 groups with methyl (CH_3) groups at the end (*n*-alkanes). They can have one or more alkyl side chains (branched and isoprenoid alkanes), or they can contain one ring or several rings (cyclic and polycyclic alkanes). Several of the polycyclic saturated alkanes like (tetracyclic) steranes and pentacyclic triterpanes are classified as biomarkers. Their presence and relative abundance as well as their remarkable stability under weathering allow their use as fingerprints to gain information on the origin of crude oils and to distinguish crude oils from different sources (for fundamental background and overviews see, e.g., Mackenzie, 1984; Brocks and Pearson, 2005; Peters et al., 2005b; Gaines et al., 2009; Brocks and Summons, 2014; Stout and Wang, 2018). Biomarkers (also termed biological markers, molecular fossils, fossil molecules, or geochemical fossils) are organic compounds in natural waters, sediments, soils, fossils, crude oils, or coal that can be unambiguously linked to specific precursor molecules biosynthesized by living organisms. The main reason for this specificity is that the bonds to the four neighboring atoms (carbon or hydrogen) are sterically oriented (tetrahedral). Thus, the rings are not planar as in aromatic hydrocarbons, but rather have a (sometimes slightly skewed) three-dimensional chair or boat configuration. Biosynthesis leads to specific steric orientation of several bonds in the biomarkers (chiral centers, optical activity). The orientation of some of these chiral centers is altered during the geothermal transformation of organic matter in petroleum source rocks (stereoisomerization) into thermodynamically more stable species, providing clues to the geothermal history (maturation) of the organic matter.

Aromatic hydrocarbons (Figures 2 and 3) contain one or more hexagonal, six-carbon ring structures with the equivalent of three conjugated double bonds; in reality, the electrons are not localized in three separate bonds but are shared among the six carbon atoms. As a consequence of the specific bond type, aromatic hydrocarbons are planar. In heteroaromatic compounds, a carbon atom in the six-membered ring is replaced by a nitrogen atom (e.g., pyridinic species). Other heteroatom-containing compounds in petroleum have a sulfur, a nitrogen, or, less commonly, an oxygen atom in a conjugated five-membered ring, either alone or adjacent to one or more aromatic ring(s). These classes of compounds are known as thiophenic (sulfur), pyrrolic (nitrogen), or furanic (oxygen). The term "aromatic" stems from the fact that many naturally occurring compounds that contain aromatic rings have distinctive scents. Polycyclic aromatic hydrocarbons (PAHs) have two or more fused aromatic rings and can be quite large. PAHs occur in petroleum and form by incomplete combustion of organic matter. They are common air and water pollutants. They can be toxic, carcinogenic, or mutagenic, and are relatively persistent in the environment. While most aromatic hydrocarbons in petroleum carry one or more alkyl substituents (methyl groups or longer alkyl chains such as those in the alkylated homologues of naphthalene, phenanthrene, dibenzothiophene, fluorene, and chrysene; Figure 2), products of incomplete combustion are predominantly unsubstituted (parent) PAHs (Figure 3; see Yang et al., 2014, for a recent overview). In this respect, the aromatic hydrocarbon composition of petroleum differs from that in products of incomplete combustion like those from oil that is burned during spill mitigation.

Resins (also called heterocompounds or N,S,O-compounds) are the most polar maltene fractions obtained by liquid chromatographic separation of crude oils. The precise chemical structures of most of the individual components are ill-defined, but the elevated polarity of the resin fraction is due to the presence of heteroatoms like nitrogen, sulfur, oxygen, and metals (as in the petroporphyrins; Figure 1), as well as the larger molecular size of many of the compounds. Resin fractions are not commonly analyzed in

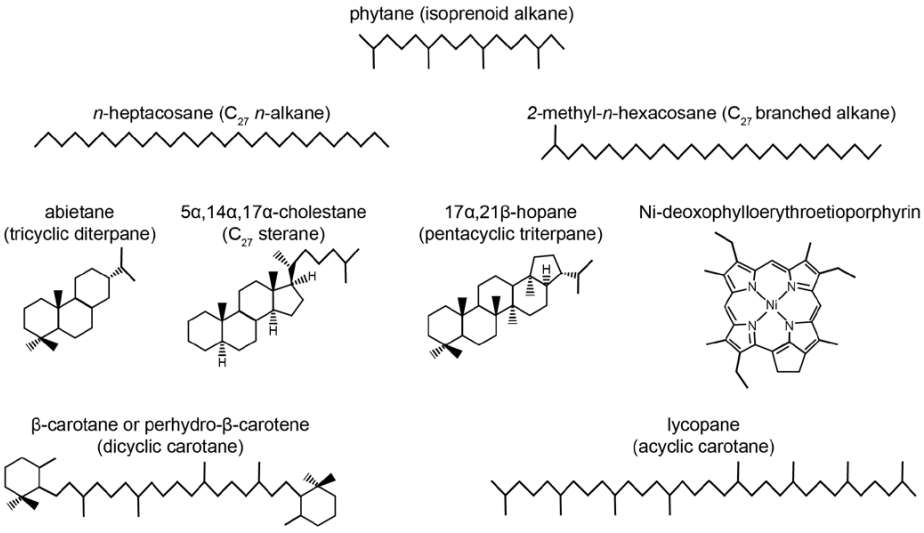

FIGURE 1. Examples of common saturated hydrocarbon biomarkers and a nickel porphyrin in crude oils.

detail, but their relative proportions are determined gravimetrically.

Asphaltenes, the most polar fraction of crude oils, can be extracted from sedimentary rocks rich in organic matter by polar solvents as part of the total extract (bitumen). They are defined by their insolubility in alkane solvents (i.e., *n*-pentane or *n*-heptane) but solubility in aromatic solvents (i.e., benzene or toluene). In chemical composition (in particular, molecular size and polarity), asphaltenes are intermediate between resins and kerogen, the insoluble high-molecular-weight organic matter in petroleum source rocks. Representations of possible asphaltene molecular structures are found in the literature, but are highly speculative (e.g., Rullkötter and Michaelis, 1990; Snowdon et al., 2016). Asphaltenes are obtained by precipitation of a solution of crude oil in a small amount of a polar solvent following the addition of excess nonpolar solvent (*n*-pentane or *n*-heptane) before liquid chromatographic separation. The yields are solvent dependent (i.e., the less polar solvent *n*-pentane yields higher amounts of asphaltenes than the slightly more polar *n*-heptane). Thus, all these subfractions of crude oil are defined by the procedures used to separate them as well as by their chemical natures.

Quantities Released During the Deepwater Horizon Oil Spill

Quantification of oil and gas released over an 87-day period after the DHW accident from the Mississippi Canyon Block 252 (MC252) reservoir of mid-Miocene turbiditic sand was not straightforward. It required a combination of measurements, calculations, and mathematical modeling. According to the information provided in the review by Kujawinski et al. (2020), the broken well released 530,000 tonnes of oil (defined as hydrocarbons with six or more carbon atoms that are liquid at ambient pressure). In addition, 170,000 tonnes of natural gas (hydrocarbons with five or less carbon atoms that are gases at ambient pressure) escaped near the seafloor, in 1,500 m water depth at high pressure and with a temperature of about 100°C, into the overlying cold water column (Reddy et al., 2012; note that these amounts are approximate, and slightly different numbers can be found elsewhere in the literature; according to Lee et al., 2018, a federal court ruled in January 2015 that "BP was liable for 3.19 M barrels of crude oil that leaked into the Gulf" of Mexico).

The "live oil," a technical term used by the petroleum industry for the reservoir-derived mixture of gaseous and liquid petroleum components, was affected right after its release due to the change in pressure and temperature. Extensive dissolution of particularly the gaseous hydrocarbons in the deep sea (Kessler et al., 2011; Valentine et al., 2010) occurred in the subsurface plume at around 1,100 m water depth. Thus, according to Reddy et al. (2012), differences in calculated total amounts of petroleum released by various investigators are most likely due to different assumed gas-to-oil ratios (GOR). These different assumptions in turn relate back to variations in the composition of samples affected to different extents by dissolution processes (e.g., see differences in GOR in the two samples in Table 2).

The remainder of the petroleum reached the sea surface, where 140,000–200,000 tonnes of the volatile compounds (about up to the volatility of *n*-hexadecane) evaporated into the atmosphere within 3–10 h of surfacing (Gros et al., 2017; Ryerson et al., 2012; Drozd

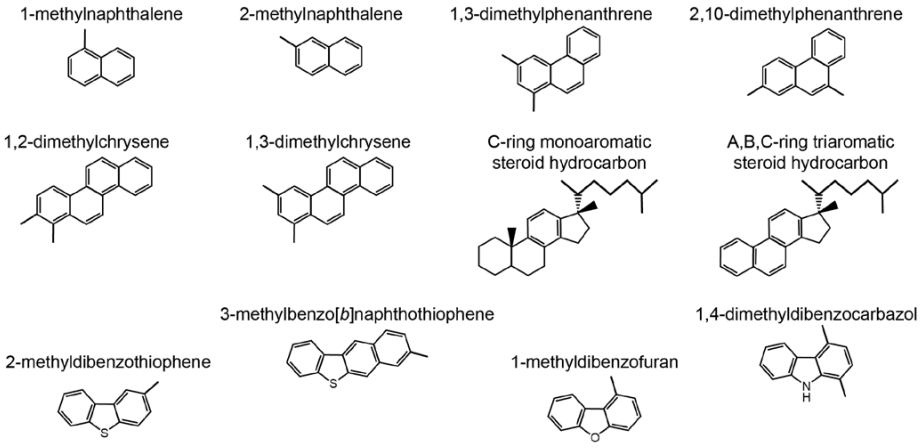

FIGURE 2. Examples of structures of alkylated aromatic hydrocarbons, aromatic hydrocarbon biomarkers, and alkylated heterocyclic aromatic hydrocarbons in crude oils.

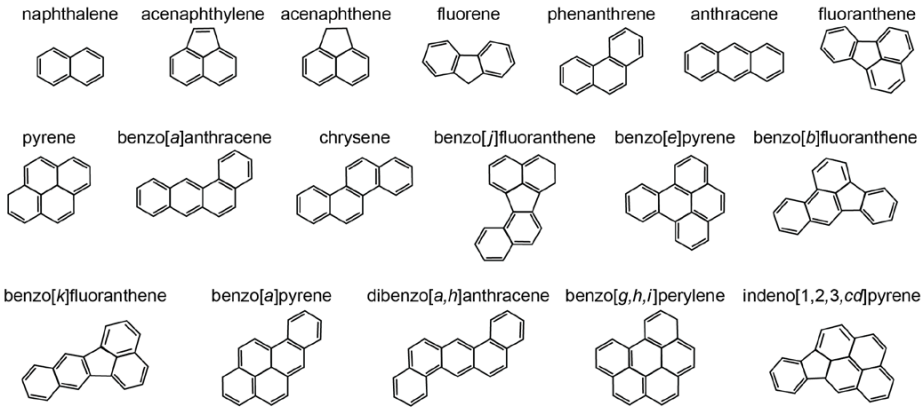

FIGURE 3. Sixteen US Environmental Protection Agency parent polycyclic aromatic hydrocarbons (PAHs) plus benzo[*j*]fluoranthene and benzo[e]pyrene.

et al., 2015) and 330,000–360,000 tonnes of the less volatile compounds spread over 11,000 ± 5,000 km^2 (Ryerson et al., 2012; Drozd et al., 2015; McDonald et al., 2015; Gros et al., 2017), reaching a total of 2,000 km of coastline along five Gulf of Mexico states (Nixon et al., 2016). Approximately 2%–20% of the total released hydrocarbons were deposited on the seafloor (Passow and Stout, 2020), primarily as oil residue. In response to the disaster, 2.9 million and 4.1 million liters of chemical dispersants were applied at the wellhead near the seafloor and at the sea surface, respectively (Lehr et al., 2010). These efforts to sequester oil in the deep sea and reduce surface oil slicks used quantities of dispersants higher than during any other known application in history (for more information on dispersants, see Quigg et al., 2021, in this issue). In total, the unintentional DWH oil release and its mitigation were unprecedented by almost any metric of marine oil discharge disasters, including in terms of volume and scale of hydrocarbon release, depth of the discharge, and application of surface and subsurface dispersants. Only the war-related intentional destruction of oil installations during the Iraqi invasion into Kuwait near the Arabian-Persian Gulf in 1990 released more petroleum into the ocean (Tawfiq and Olsen, 1993).

TABLE 2. Composition of hydrocarbon gases (C_1 to C_5) and oil sample MW-1 collected from the Macondo well on June 21, 2010 (Reddy et al., 2012), and a comparison of gas end members estimated from field data collected by Valentine et al. (2010).

ANALYTE	MW-1 CONTENT	VALENTINE ET AL. (2010)[a]
GAS[b]		
Methane	82.5% ($\delta^{13}C$ = −57.5‰; δD = −187‰)	87.5% ($\delta^{13}C$ = −61.3‰)
Ethane	8.3% ($\delta^{13}C$ = −31.5‰; δD = −147‰)	8.1%($\delta^{13}C$ = −30.5‰)
Propane	5.3% ($\delta^{13}C$ = −29.2‰; δD = −123‰)	4.4% ($\delta^{13}C$ = −29.0‰)
Isobutane	0.97% ($\delta^{13}C$ = −29.9‰)	NA
n-Butane	1.9% ($\delta^{13}C$ = −27.9‰; δD = −119‰)	NA
Isopentane	0.52%	NA
n-Pentane	0.52%	NA
Methane/ethane	9.9	10.85
Methane/propane	15.5	19.8
GOR (measured)	1,600 standard cubic feet per barrel	NA
GOR (estimated)	1,730 standard cubic feet per barrel[c]	NA
GOR		3,000 standard cubic feet per barrel[d]
OIL (SELECT PROPERTIES)[e]		
Density	820 g L^{-1}	NA
Gravity	40° API	NA
Carbon	86.6%	NA
Hydrogen	12.6%	NA
Nitrogen	0.38%	NA
Sulfur	0.39%	NA
Saturated hydrocarbons	74% ($\delta^{13}C$ = −27.9‰)	NA
Aromatic hydrocarbons	16% ($\delta^{13}C$ = −26.5‰)	NA
Polar hydrocarbons	10%	NA

GOR = Gas-to-oil ratio; NA = not applicable

[a] Valentine et al. (2010) defined only the relative abundances for the endmembers methane, ethane, and propane from field samples. The relative percentages of hydrocarbon gases measured in MW-1 were calculated using methane through pentanes.

[b] Reddy et al. (2012) measured butanes and pentanes in both the gas and oil in MW-1. Here, only the butanes and pentanes isolated in the gas fraction are shown. For a complete accounting of all compounds collected, see supplementary material in Reddy et al. (2012).

[c] Estimated from Mango ratios (Jarvie et al., 2015) using the composition of 2- and 3-methyl pentanes and 2- and 3-methyl hexanes in MW-1 oil (Table S2 in Reddy et al., 2012)

[d] Valentine et al. (2010) chose this value based on "information released by BP."

[e] See SI text in Reddy et al. (2012) for discussion of properties listed in this section of the table.

Physical Properties and Chemical Composition of Macondo Oil

Oil droplets released during the Macondo oil spill occurred in three size categories, each with different buoyancies but with overlapping chemical compositions (Ryerson et al., 2012). Oil droplets greater than 0.3 mm diameter exhibited sufficient buoyancy to rise to the ocean surface in less than four hours (Ryerson et al., 2012), transporting a mixture of soluble and insoluble compounds, some of which volatilized into the atmosphere (Ryerson et al., 2011; de Gouw et al., 2011). The medium-sized droplets (0.1–0.3 mm) ascended more slowly (rise times below 10 h), and their behavior was very sensitive to initial oil composition and release dynamics. For example, moderately soluble hydrocarbons such as toluene, xylene, naphthalene, cyclopentane, and methylcyclopentane partitioned to the aqueous phase from all droplet sizes as a function of the droplets' exposure time and surface area-to-volume ratio, as well as their relative concentrations in the oil (Ryerson et al., 2012). In contrast, droplets smaller than 0.1 mm and soluble gases (methane, ethane, propane) lacked the buoyancy to rise after being emplaced in deep-sea intrusions, although the degree of hydrocarbon dissolution could not be measured due to challenges in separating oil droplets from the surrounding water (Ryerson et al., 2012). A substantial fraction of the released oil and gas (by mass) was retained in the deep-sea intrusions because of the relatively high proportion of gases in the DWH blowout. However, reducing the sea surface concentrations of released hydrocarbons was a high priority during DWH spill mitigation. Thus,

responders decided to convert the larger, faster-rising oil droplets into small droplets that would remain in the deep sea applied chemical dispersants directly at the outflow near the seafloor.

Overton et al. (2016), Kujawinski et al. (2020), and Oldenburg et al. (2020) included bulk and molecular information on the Macondo oil in their reviews of the chemical analysis of original and transformed petroleum spilled during the DWH incident at mid-term and toward the end of the Gulf of Mexico Research Initiative (GoMRI), respectively. Petroleum sampled directly above the Macondo well during the blowout ("live oil"; Table 2) was determined to have a GOR of 1,600 standard cubic feet per barrel petroleum (Reddy et al., 2012). Valentine et al. (2010) and Reddy et al. (2012) both reported the gas being composed of mainly methane (87.5% and 82.5%, respectively) and smaller amounts of ethane (abundance just above 8%) and propane (around 5%). The ^{13}C and ^{2}H stable isotope contents increased with increasing carbon number of the gases (Table 2), indicating generation of the hydrocarbons from mature organic matter in the petroleum source rock (cf. Sherwood Lollar et al., 2002). Reddy et al. (2012) assessed the Macondo oil as a light oil (API gravity 40° with a density of 820 g L^{-1}), whereas Daling et al. (2014) reported that the oil collected through the riser insertion tube tool (RITT) on the drillship *Discoverer Enterprise* on May 22, 2010, had a density of 833 g L^{-1}, a pour point of −27°C, and an interfacial tension of 20 mN m^{-1} (millinewtons per meter). The initial viscosity of the Macondo oil was evaluated to be 3.9 cP at 32°C (Daling et al., 2014). The relative distribution of compound groups of the pyrrolic N1 heteroatom class, namely, double bond equivalent (DBE) 9 (alkylated carbazoles), DBE 12, and DBE 15 (alkylated benzo- and dibenzocarbazoles, respectively) as established by Oldenburg et al. (2014) indicated a maturity level of 0.9% vitrinite reflectance equivalent ($\%R_e$) for the Macondo oil. This is consistent with $\%R_c$ of 0.94 calculated from the Methyphenanthrene Index 1 (MPI-1; Radke and Welte, 1983) based on the relative PAH concentrations displayed in Figures 2 and 3 of Overton et al. (2016). Both values render the Macondo oil moderately mature near the peak of oil generation, consistent with the stable isotope composition of the gases (Table 2).

Reddy et al. (2012) found the nonbiodegraded Macondo oil to be dominated by saturated hydrocarbons (74%), followed by aromatic hydrocarbons (16%) with the non-hydrocarbon (polar) fraction comprising 10%. The authors reported that the GC-MS amenable Macondo oil composition (C_5 to C_{38} saturated and aromatic hydrocarbons) was dominated by branched alkanes (26%), followed by cycloalkanes (16%) and *n*-alkanes (15%), and that aromatic species such as alkylbenzenes and indenes (9%) and polycyclic aromatic hydrocarbons (4%) were less abundant. The GC-MS amenable content of polar oil constituents was 10% (e.g., dibenzothiophenes), with sulfur and nitrogen elemental abundances of the Macondo oil assessed as 0.4% each.

Mass chromatograms of saturated hydrocarbon biomarkers in the Macondo oil (Overton et al., 2016) show the typical distribution pattern of thermally stable 17α-hopanes (*m/z* 191, displayed in the C_{27} to C_{33} range of pseudohomologues) and steranes (*m/z* 217), indicating generation from a source with a clastic rock matrix (due to significant amounts of diasteranes, or rearranged steranes; e.g., Mello et al., 1988) and moderate maturity of the oil (based on the amount of 5α,14β,17β- relative to 5α,14α,17α-steranes; Mackenzie, 1984; Seifert and Moldowan, 1986). The PAH distribution patterns, besides moderate amounts of the respective parent hydrocarbons, exhibit a prominent series of alkylnapthalenes followed in abundance by alkylphenanthrenes, alkyldibenzothiophenes, alkylpyrenes and alkylchrysenes (Overton et al., 2016).

As only a very small percentage of the non-hydrocarbon (polar) fraction is GC-amenable due to high boiling points, Fourier-transform ion cyclotron resonance mass spectrometry (FT-ICR MS) was the analytical method of choice to study this oil fraction. McKenna et al. (2013) characterized more than 30,000 acidic, basic, and nonpolar unique neutral elemental compositions for the Macondo crude oil constituents (see below). However, while certain chemical characteristics of these compounds are known, the exact chemical structures are not yet elucidated. That is a challenge going forward.

Analytical Techniques for Oil Spill Sample Analysis

The challenge of analyzing crude oil of any origin, native or altered, arises from the complexity of this substrate on the molecular level. Attempts made many decades ago to achieve a complete inventory of all constituents of petroleum (Rossini and Mair, 1959; Smith, 1968) turned out to be illusory. The task is to simplify the mixture by fractionation and then search these fractions for characteristic components of high significance, such as biological markers as indicators of origin or selected PAHs as indicators of source and/or toxicity. White et al. (2016a) provided a helpful review of the analytical chemistry used to study the Macondo oil and samples taken to study the fates and effects processes. We present a brief synopsis and an update of what has been learned since that review.

Fractionation uses "dead oil" (i.e., the most volatile components have been evaporated so that they do not interfere with gravimetric determination of the proportions of the separated fractions). The process starts with removal of asphaltenes (as described earlier), which may otherwise precipitate during chromatography and cause bad separation performance.

Column chromatography, a technique for separating mixtures of organic compounds, involves dissolving the mixtures in a mobile phase and passing them through a column filled with a stationary phase. Compounds in the mixture

have different affinities for the mobile and stationary phases. They are adsorbed onto the stationary phase and then, as the mobile phase flows through the column, separated and sequentially released and collected. A compound's residence time in the column depends on the stationary and mobile phases, and its boiling point, molecular size, molecular shape, and polarity. Column chromatography refers to the use of a vertical glass column filled with silica gel or aluminum oxide, as stationary phase; an organic solvent dripped into the top of the column, as mobile phase; slow percolation through the column under the force of gravity; and separated groups of compounds collected as they drip out the bottom. In a more general sense, thin-layer chromatography (TLC), medium-pressure liquid chromatography (MPLC), high-performance liquid chromatography (HPLC), and preparative gas chromatography (prep GC) are forms of chromatographic separation with different stationary and mobile phases (e.g., Vitha, 2016). This initial step is occasionally followed by further fractionation including separation of straight-chain, branched, and cyclic saturated hydrocarbons by (thio)urea adduction or application of zeolites with different pore sizes (e.g., Peters et al., 2005a), or by separation of aromatic hydrocarbons into classes of different ring numbers (e.g., Radke et al., 1984).

Even after fractionation, the identification of individual constituents of crude oils and related substances is not straightforward. A breakthrough in the 1970s was the development of capillary columns a few tens of meters in length and internally coated with different types of silicone oil as stationary phases. Shortly after, this was followed by the construction of devices for coupling such columns to fast-scanning mass spectrometers with connected computers for data processing. Continuous development of the gas chromatography-mass spectrometry (GC-MS) technique over about two decades was the basis for a rapid increase in understanding of the molecular composition of organic matter in sedimentary rocks and petroleum, and of changes in its composition as a function of geological and environmental conditions.

The straight-chain alkanes (*n*-alkanes) and isoprenoid alkanes pristane and phytane that are abundant in most unaltered crude oils can be identified and quantified by gas chromatography with flame ionization detection (GC-FID; e.g., Peters et al., 2005a). (This rarely applies to other compounds, which may not have the regular retention time pattern on a GC column or are abundant enough for easy detection.) They require the power of mass-specific detection and benefit from the fact that entire groups of saturated hydrocarbon biomarkers have a common mass spectrometric key fragment. Thus, mass chromatograms, which by a factor of about 30 are more sensitive than entire mass spectra, reveal the presence of the full range of these compounds (e.g., Peters et al., 2005b; Overton et al., 2016). An even further advanced mass spectrometric detection technique, mass fragmentography (GC-MS-MS), further increases the sensitivity by another factor of up to five and is also more compound-specific than mass chromatography (e.g., Summons et al., 1999; He et al., 2018).

Similarly, comprehensive two-dimensional gas chromatography (GC×GC) increases the resolution of complex mixtures. Gaines et al. (1999) published an early application of this technique to a marine oil spill. Using two sequentially coupled gas chromatographic columns with different separation efficiencies related to molecular properties (e.g., volatility and polarity), GC×GC produces a two-dimensional retention surface, which significantly improves compound identification compared to the one-dimensional retention data of a normal GC column. Compounds with similar chemical structures are grouped together in the chromatogram, allowing rapid preliminary identification with even minor components being separated and detectable. The GC×GC technique considerably matured scientifically in the course of the GoMRI research. It was intensely used to examine changes in the abundance of Macondo oil constituents, and the products were ascribed to various categories of physical and chemical weathering (e.g., Hall et al., 2013; Aeppli et al., 2014, 2018; Gros et al., 2014, 2016).

The two-dimensional retention surfaces from GC×GC analysis of crude oils and their transformation products after an oil spill, despite the additional dimension of separation, are still very complex. Figure 4 illustrates the principles of this technique for a simple case study. Aeppli et al. (2013) analyzed oil sheens that were first observed in September 2012 close to the DWH disaster site more than two years after the Macondo well had been sealed. Linear unsaturated alkenes common in synthetic drilling fluids led them to identify an 80-ton cofferdam, abandoned during the operation to control the Macondo well in May 2010, as the source of the sheens. Figure 4a–d compares the GC×GC data for the cofferdam oil, an oil sheen sample, the hydrogenation product of the oil sheen sample, and drilling mud from the multi-purpose supply vessel *HOS Centerline*, which supplied drilling mud during the Top Kill and Static Kill operations at the DWH site. The more polar alkenes occur slightly higher on the second dimension separation (y-axis) than the *n*-alkanes. The white dashed lines in the four diagrams denote the surface where drilling-mud olefins elute. The compounds have disappeared in the oil sheen hydrogenation product because the alkenes were transformed into *n*-alkanes (see Figure 4 caption).

Even with the expanded compositional information from GC×GC (Hall et al., 2013), GC-based techniques are unable to detect many oxidation products, notably those that are highly oxidized with boiling points or thermal stabilities outside of the GC range (Aeppli et al., 2018). As determined through ultrahigh resolution mass spectrometry (FT-ICR MS), elemental assignments for tens of thousands of molecules in the native (unaltered) and weathered Macondo oil revealed the

chemical changes induced by weathering (Figure 5d; Ruddy et al., 2014). Subsequent analysis of different crude oil fractions (oil-soluble non-interfacially active, oil-soluble interfacially active, and water soluble) indicated that decreasing carbon and increasing oxygen numbers determined the progression of molecules from oil-soluble to water-soluble (Zito et al., 2020). Thus, weathering-induced chemical changes (see arrows in Figure 5) were linked to changes in oil solubility. Both the oil- and water-soluble photo-transformed species span aliphatic to highly aromatic structures (Ruddy et al., 2014; Niles et al., 2019), indicating that these products originate from both aliphatic and aromatic hydrocarbon precursors (Hall et al., 2013). These results suggest that both direct and indirect photo-oxidation contributed to the generation of most of the transformation products identified in field samples. Thus, FT-ICR MS developed into an extremely powerful technique for analyzing high-molecular-weight and polar constituents of crude oil and its transformation products within GoMRI research and for an understanding of the fate of petroleum during weathering.

FT-ICR MS was responsible for only part of the progress made in molecular insight into oil spill processes. The complexity of oil required a suite of analytical tools to comprehensively explore weathering mechanisms and products (Figure 5a–d). In addition to the GC-based and FT-ICR MS tools described above, thin-layer chromatography-flame-ionization detection (TLC-FID; Aeppli et al., 2012) and Fourier-transform infrared spectroscopy (FT-IR; White et al., 2016b) provided quantitative and informative estimates of functional group changes from weathering processes.

Evans Seeley et al. (2018) followed a different route to unravel the complexity of weathered petroleum from the DWH oil spill. They explored the analytical capabilities of ramped pyrolysis-gas chromatography–mass spectrometry (py-GC–MS) and showed that bulk-flow py-GC–MS can quantify the overall degree of petroleum hydrocarbon weathering. Furthermore, thermal slicing py-GC–MS can quantify specific compounds in the "thermal desorption zone" (50°–370°C), as well as characterize pyrolyzed fragments from non-GC-amenable petroleum constituents (including oxidation products) in the "cracking zone" (370°–650°C). Their data suggest an increase in thermodynamic stability, concentration of oxygenated products, and complexity of high-molecular-weight and/or polar components with advanced weathering. Wang et al. (2020) further applied this approach to gain insight into formation mechanisms and structures of some of the asphaltenes generated by photo-oxidation.

Stable carbon and hydrogen isotopes are widely used to characterize crude oils and their constituents (cf. Table 2). For tracing the fate of the Macondo oil spilled during the DWH disaster (i.e., mixing with organic matter of recent origin on the seafloor or the incorporation of carbon from the microbial transformation of Macondo oil components into biomass and food webs), measurement of the radioactive carbon (^{14}C) contents of sedimentary and biological substrates was the method of choice. Because it has been so long since the petroleum source organic matter was buried and transformed from plant biomass into petroleum, the ^{14}C isotopic content of petroleum is zero when compared to recently produced plant biomass (Chanton et al., 2015). Thus, radiocarbon contents lower than those of fresh biomass indicate mixing with petroleum-derived carbon.

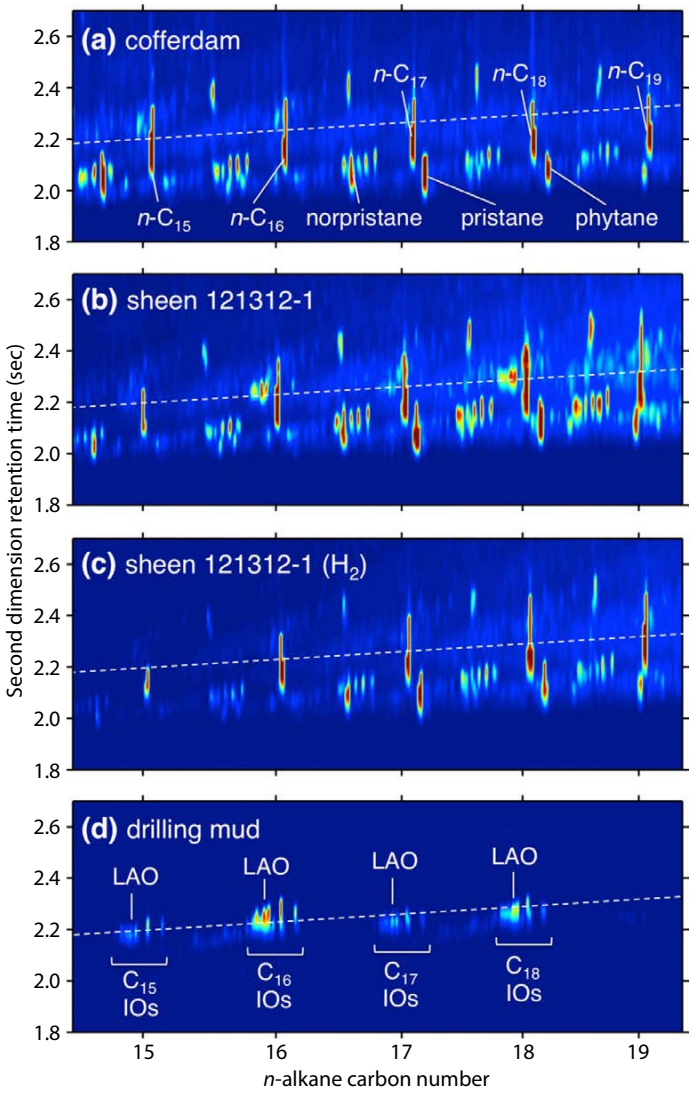

FIGURE 4. Partial two-dimensional gas chromatography flame-ionization detection (GC×GC-FID) chromatograms of (a) cofferdam oil, (b) oil sheen 121312-1, (c) hydrogenated oil sheen 121312-1, and (d) drilling mud from the multi-purpose supply vessel *HOS Centerline*. White dashed lines denote the surface locations where drilling-mud olefins elute. The sum of the C_{16}-, C_{17}-, and C_{18}-olefins relative to the whole FID signal was 1.2% in the sheen sample (b) and not detectable in the cofferdam oil (a). The olefins in the sheen sample disappeared upon hydrogenation and exhibited a pattern like that of pure drilling mud, which represents an isomer mixture of C_{15} to C_{18} internal olefins that includes one linear α-olefin per carbon number. The data are displayed as color contour plots, with blue representing low signal, yellow representing medium signal, and red representing high signal. In order to visualize minor peaks, the plotted dynamic range is less than the total dynamic range of the sample, with the intensity saturated near the point of maximum elution. *Reprinted with permission from Aeppli et al. (2013). Copyright 2013 American Chemical Society*

As summarized by Kujawinski et al. (2020), dioctyl sodium sulfosuccinate (DOSS) was used to track the fate of the deep-sea dispersants applied for spill mitigation during the DWH disaster; this compound was selected because it comprises a large and relatively constant fraction of Corexit and other dispersant formulations, and it was amenable to existing analytical protocols. Samples taken during and a few months after the disaster indicated that DOSS persisted in the subsurface intrusion and was not degraded (Kujawinski et al., 2011), contrary to expectations based on laboratory experiments performed under surface conditions (Baelum et al., 2012). These data suggest that some of the chemical dispersant components were not degraded appreciably in the deep sea in the aftermath of the DWH disaster. Subsequent laboratory work showed that DOSS was less labile than the solvent carriers in the dispersants under deep-sea conditions (Baelum et al., 2012), and others found minimal degradation of DOSS at low temperatures (Campo et al., 2013), further supporting this conclusion.

IN SITU BURNING OF OIL AT THE SEA SURFACE

In situ burning (ISB) of spilled oil on the surface of the water (see photo on first page of this article) is controversial because of concerns about chemicals produced and/or released to the atmosphere during the burn process and concerns about the chemicals left in the unburned residues at the water-atmosphere interface or in the unburned slick (Stout and Payne, 2016). During the DHW spill response, an estimated 220,000–313,000 barrels of oil at the ocean's surface were removed during 411 carefully conducted ISB operations. This estimated 5% of the spilled oil (Schaum et al., 2010) is considered to have "played a significant role in reducing the amount of oil on the water's surface" (NOAA Office of Response and Restoration, 2020). For comparison, the 5% Macondo oil removed by ISB is roughly equal to the estimated total oil released during the 1989 *Exxon Valdez* tanker accident (Stout and Payne, 2016).

The ISB operations were informed by experience gained between the 1970s and 2010 from laboratory tests, controlled field experiments, and a few oil spill responses (e.g., Fritt-Rasmussen and Wegeberg, 2015; Gullet et al., 2017; Bullock et al., 2019, and references therein). The different mixes of gas and oil and their variable compositions, and environmental conditions such as temperature and wind, can influence the efficiency of ISB and the composition of products formed. Burning of oil yields mainly carbon dioxide and water. According to a liter-

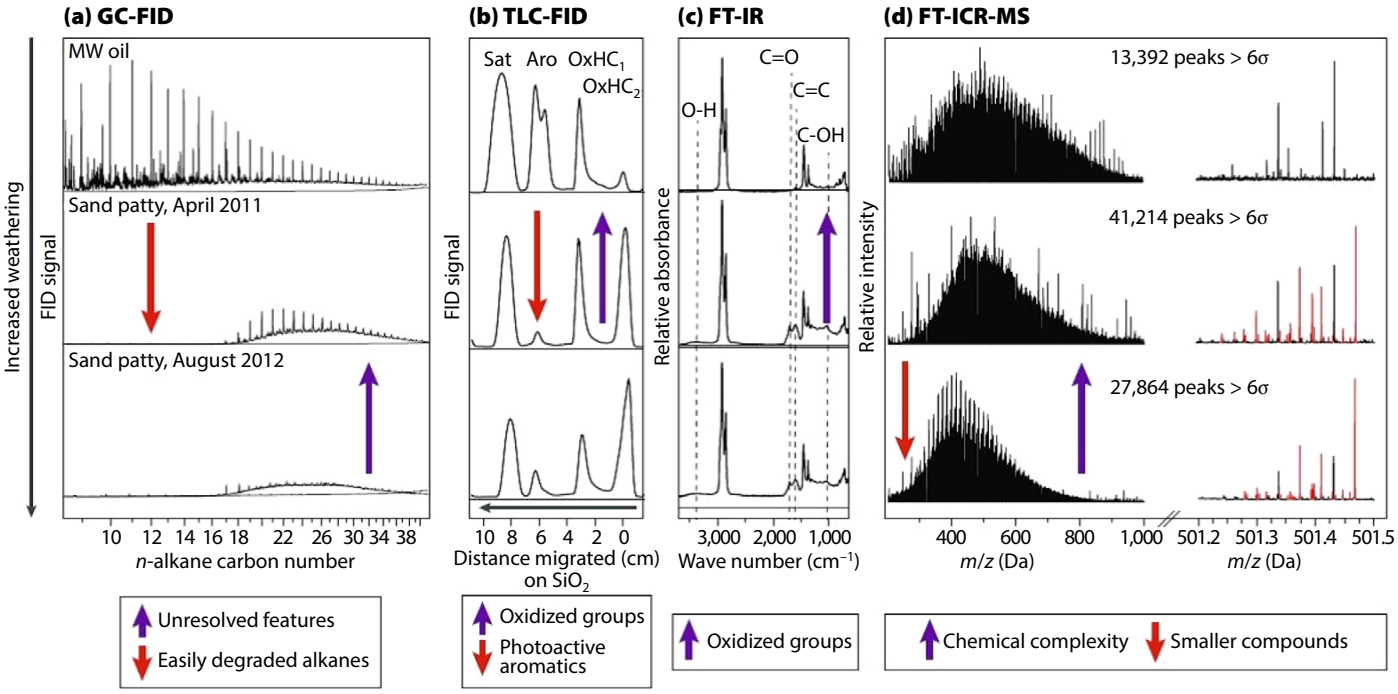

FIGURE 5. Analysis of Deepwater Horizon oil and field sample chemical compositions. Four different techniques capture the collective effects of abiotic and biotic weathering on oil (initial oil spectra along top row), which are manifested in changes of: (a) gas chromatography flame-ionization detection (GC-FID) chromatograms, (b) thin-layer chromatography flame ionization detection (TLC-FID) chromatograms, (c) Fourier transform-infrared (FT-IR) absorbance, and (d) broadband Fourier transform ion cyclotron resonance mass spectrometry (FT-ICR MS) spectra. Field samples include sand-oil patties collected from Gulf of Mexico beaches. Overall, weathering led to degradation of saturated and aromatic compounds leaving recalcitrant compounds in the unresolved complex mixtures, an increase in oxidized hydrocarbon (OxHC) fractions relative to saturated and aromatic hydrocarbon compounds, and increases in hydroxyl and carbonyl functional groups. The negative ion mode ESI FT-ICR MS revealed a complexity increase in the number of peaks (from *m/z* 200–1,000), and the appearance of oxygenated species (red peaks) in a mass-scale expanded 400 mDa segment at 501 Da. Similar molecular information is available for all other nominal masses in the mass spectrum. *Reprinted from Kujawinski et al. (2020) with permission from Springer Nature; panels a–c were adapted from Aeppli et al. (2012) with permission from the American Chemical Society*

ature compilation of different oil burning experiments using various substrates (Booher and Janke, 1997, mostly based on the work of D.D. Evans, National Institute of Standards and Technology, in the early 1990s), products of burning oil, excluding water, are about 92% carbon dioxide, 3.2% carbon monoxide, 4.6% smoke (soot/black carbon), 0.03% PAHs, and 0.27% volatile organic chemicals (VOCs). Of the VOCs, about 0.14% are C_2-C_6 hydrocarbons and 0.12% are C_1-C_{16} aldehydes/ketones (organic compounds escaping complete combustion), 0.9% SO_x and 0.0004% NO_x (Figure 6a).

Gullett et al. (2017) performed laboratory-scale experiments by burning representative crude oil in two outdoor pans with areas of 0.47 m^2 and 0.93 m^2. The pans were filled with seawater and a Strategic Petroleum Reserve Bayou Choctaw Sweet crude oil reported to have chemical composition and physical characteristics similar to that of the Macondo oil. They measured 82% carbon dioxide, 2.5% carbon monoxide, 7.0% total particulate matter, 0.34% volatile organics, and 0.10% PAHs in the resulting smoke (Figure 6b), but because 7.6% of products were not accounted for among the components listed, the differences from the Booher and Janke (1997) compilation are not substantial.

US NOAA aircraft-based measurements during active surface burning of Macondo oil slicks led to estimates of 4% of the burned material or an estimated 1.35 ± 0.72 thousand tonnes released as black carbon into the atmospheric plume (Perring et al., 2011). Those authors reported the black carbon particles had little non-refractory material and were typical of black carbon from fairly efficient fossil fuel burning.

The combustion products of main concern were residues of black carbon and other components of soot. Most attention focused on PAHs formed during combustion and associated with the soot and black carbon. Combustion-derived PAHs have an overlapping chemical composition with PAHs native to crude oils. Numerous studies have shown that PAHs from combustion sources contain more of the parent, non-alkylated PAHs compared to crude oils and fuel oils, with the predominance of the parent, non-alkylated PAHs increasing with higher temperatures of combustion (e.g., Lima et al., 2005). The composition of the PAHs associated with the soot and black carbon were assessed by several studies that measured mainly a number of parent PAHs in the molecular range of naphthalene through benzo[*ghi*] perylene (e.g., Gullett et al., 2016, 2017). Insights into the general mechanisms of rapid molecular clustering that could lead from combustion-formed PAHs to black-carbon soot in general are provided by Johansson et al. (2018).

There is a paucity of published data for the chemical composition of ISB residues (i.e., the tarry, flakey-like material found floating at the surface near or in oil slicks subjected to ISB). This is understandable. Air sampling and the smoke plume have taken priority in the past because of human health concerns (see Sandifer et al., 2021, in this issue, regarding factors that are considered in response options). Thus, it is fortunate that Stout and Payne (2016) collected two not-yet-cooled floating ISB residues immediately after ISB events. They also collected three ISB residues from the seafloor between 1,400 m and 1,440 m depth using coring and slurp gun samplers mounted on a remotely operated vehicle. All samples analyzed by gas chromatography and gas chromatograph-mass spectrometry showed some percent enrichment of pyrogenic PAHs mixed with unburned, relatively fresh Macondo oil when compared to samples of DWH oil slicks not subjected to extensive weathering. One ISB residue from the seafloor appeared to contain some admixed diesel fuel-like lower-molecular-weight hydrocarbons. The other two samples were similar in hydrocarbon composition to the ISB residues collected at the sea surface.

Stout and Payne (2016) estimated that most or all ISB residues eventually sank to the seafloor. ISB residues and their associated PAHs added to the uptake of toxic

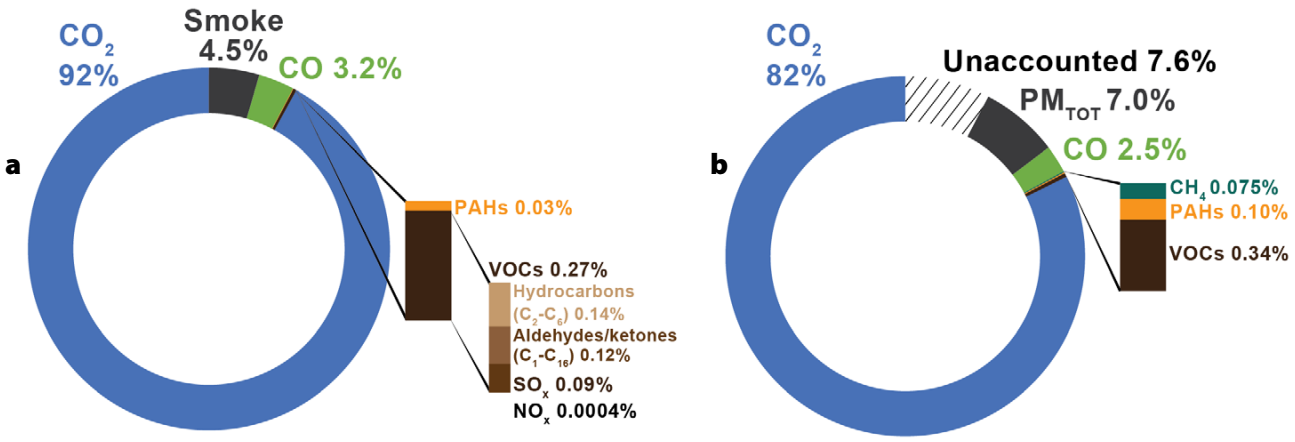

FIGURE 6. Fate of combusted oil into products (excluding water), by weight. (a) Percentages adapted from a literature compilation of Booher and Janke (1997). (b) Percentages of combustion products from experimental burning of a Strategic Petroleum Reserve Bayou Choctaw Sweet crude oil with reported chemical composition and physical characteristics similar to that of the Macondo oil (after Gullet et al., 2017). The amount of unaccounted material affects the relative proportions of the identified products. VOCs = Volatile organic compounds. PM_{TOT} = Total particulate matter.

materials and their potential adverse effects on benthic organisms (Murawski et al., 2021, in this issue). The composition of the PAHs in the floating ISB residues indicated definite loss of PAHs of lower molecular weight (e.g., naphthalene and alkylated naphthalenes), slightly less loss of phenanthrene and alkylated phenanthrenes, and less or no loss of the higher-molecular-weight PAHs relative to 17α-hopane used as a relatively stable internal hydrocarbon standard (see earlier discussion, although 17-α-hopane during ISB may not be as stable as during geothermal transformation or weathering). The sunken ISB residues contained some increase in relative concentrations of a few higher-molecular-weight PAHs indicative of contributions of combustion product PAHs to a petroleum or oil-type PAH mixture (Stout and Payne, 2016).

A US EPA 4.0 m diameter, helium-filled aerostat-lofted instrumentation package sampled plumes of 27 surface fires of various sizes using quartz filters and also polyurethane foam (PUF/XAD2/PUF) sorbent (Aurell and Gullett, 2010; Gullett et al., 2016). The samples were analyzed for polychlorinated dibenzo-dioxins (PCDDs) and polychlorinated dibenzofurans (PCDFs). This assessment was undertaken because incomplete combustion of organic matter in the presence of chloride can form small amounts of PCDDs and PCDFs, and seawater admixed with the surface oil is potentially an abundant source of chloride. Aurell and Gullett (2010) reported that the analysis of a single composite sample resulted in an emission factor of 1.7 ng toxic equivalency (TEQ) of polychlorinated aromatics per kg of oil burned.

One unintended sampling occurred during the campaign described above when it was recognized that sail fabric of the aerostat collected fine particles that could be sampled, extracted, and analyzed for various chemicals such as PAHs (Gullett et al., 2016). The focus was the long-standing EPA Priority Pollutant PAHs (initially defined for water samples; see Figure 3) that are also common in combustion products. However, a few other PAHs were detected such as alkylated naphthalenes, methylfluorene, and methylpyrene, and their presence indicates that the sample may contain some lower-temperature combustion products.

Schaum et al. (2010) screened the low-level risks that could be attributed to "dioxin" emissions from burning of Macondo oil at the sea surface. The components of both the PCDD and PCDF groups are of serious concern for human health (e.g., Van den Berg et al., 2006). The screening level assessment by Schaum et al. (2010) indicated that human cancer risks from PCDDs/PCDFs formed during the ISB did not exceed 1×10^{-6}. They noted that US EPA "typically considers the risk range of 10^{-6} to 10^{-4} to be a range where consideration is given to additional actions." Schaum et al. (2010) found sparse sampling and analysis information on the generation of PCDDs and PCDFs prior to these studies of the Macondo oil ISB. These pioneering studies were limited in scope. However, they indicate that more studies of a similar nature under varying conditions for ISB of different types of oils are needed due to the human health risks associated with the PCDD/PCDF chemicals.

An intriguing laboratory-scale experiment of ISB of a slick on water surface was conducted by Jaggi et al. (2019) and assessed using FT-ICR MS, as described earlier. They reported that both unburned oil slicks and ISB result in the release of organic compounds to the water beneath a slick. An important finding was that ISB strongly increases the concentrations of oil-related chemicals entering the water phase as a result of production of oxidized organic compounds that are soluble in water. Jaggi et al. (2019) reported that this mixture was different in composition from the organic compounds entering the water from unburned oil in that the mixture from ISB contained significantly more condensed aromatic chemicals with varying amounts of the elements nitrogen, oxygen, and sulfur. This is an important finding that merits follow-up research in the laboratory and in the field. Jaggi et al. (2019) note: "The effect of these highly unsaturated and oxygenated organic species on oil spill fate and their ecosystem impact is currently unknown."

CHALLENGES

Analytical Chemistry Methods and Applications

The complexity of oil, including the Macondo oil, represents a challenge even with present advances in analytical chemistry. During research to elucidate the fates and effects of the DWH spilled oil (Farrington et al., 2021; Halanych et al., 2021; and Murawski et al., 2021, all in this issue), inconsistencies were noted in the various analytical methods used or in which chemicals were measured. For example, investigators might measure different sets of specific PAHs, thus complicating comparison of total PAHs from different parts of the Gulf of Mexico. The same applies to ascribing a particular type and intensity of effect to the presence of individual chemical components or types of components in the Macondo oil or weathered, transformed, and/or biodegraded oil. This is the result, in part, of researchers asking different research questions or using their preferred methods, and that poses additional problems and uncertainties. Thus, while some researchers utilized GC×GC-MS, others employed single column fused-silica capillary GC with FID or GC-MS detection.

The US National Institute of Standards and Technology (NIST) prepared a Standard Reference Material for a reasonable number of Macondo oil hydrocarbons to assist with quality control and quality assurance of analyses (NIST, 2020). Pairs of this sample and a sample of the Macondo oil that had been field-weathered (Candidate SRM 2777) were distributed to laboratories involved in GoMRI research plus several others. The report of the results of this GoMRI quality control/quality assurance laboratory intercomparison is available as a NIST report (Murray et al., 2016). It provides

a basis for assessing potential uncertainties when comparing analyses from the laboratories involved. These uncertainties are similar to those that became evident from an interlaboratory comparison published nearly two decades ago at the end of the Cooperative Monterey Organic Geochemistry Study based on rock samples from Naples Beach and Lions Head sections of the Monterey Formation and related Monterey crude oils (Isaacs, 2001). An informative and thorough discussion of the use of intralaboratory and interlaboratory quality assurance/quality control for the laboratories involved in the US NOAA DWH Natural Resource Damage Assessment analyses for petroleum compounds is available in Litman et al. (2018).

Only a few GoMRI researchers had access to or employed FT-ICR MS analyses. This most likely was due to the expense of the instrument and fewer people having familiarity with the method at the time. There are relatively few advanced high magnetic FT-ICR MS instrument facilities in the world. Fortunately, GoMRI research did involve the National High Magnetic Field Laboratory at Florida State University (https://nationalmaglab.org/user-facilities/icr). The researchers at this laboratory collaborated with several other GoMRI researchers to provide new insights into the composition of the asphaltenes and other high-molecular-weight chemicals native to the Macondo oil and also to provide key insights into photochemical reaction pathways and products of these reactions as noted in references cited previously. Despite these important insights, the exact molecular structures of these chemicals remain to be elucidated. Thus, the detailed pathways of, for example, some of the photo-oxidation reactions and their products remain a challenge.

Agencies responsible for oil spill response and assessment of the fates and effects of spills are challenged with planning for appropriate incorporation of these advanced analytical methods into their response and assessment activities.

CONCLUSIONS

Assessment of the full impact of the petroleum released during the Deepwater Horizon oil spill on Gulf of Mexico flora and fauna, and on human health in the region, requires determination of the quantities of materials that entered the environment, including the amounts of dispersants used during spill mitigation. In addition, chemical analysis of the composition of the released materials and their relative proportions are of similarly high importance.

Chemical analyses of the released petroleum and the products of physical, chemical, and biological alteration were performed using a wide range of techniques that were developed in analytical chemistry, petroleum organic geochemistry, and environmental chemistry over several decades since the 1970s. In addition, more advanced techniques like the sequential combination of two gas chromatographic columns with different separation efficiencies (GC×GC) and ultrahigh-resolution mass spectrometry (FT-ICR MS) were the methods of choice for shedding light on the complex mixtures of high-molecular-weight and very polar petroleum constituents, particularly those newly formed during photo-oxidation of liquid oil. Photo-oxidation is a very important, but hitherto underestimated, weathering process. Together, this suite of analytical methods provided not only an inventory of the most important constituents of the released petroleum but also a greater understanding of the reaction mechanisms of weathering processes such as photo-oxidation and the identity of its transformation products, as well as their impacts on physical properties, bioavailability, and toxicity of the discharged oil. Expanded understanding, combined with application of complementary analytical techniques, will inform real-time responses in future oil spills.

Finally, important insights have been gained in the past 10 years about the chemical composition of products of in situ burning of oil at the water surface. However, field assessment and laboratory data are limited, and these exciting new insights need further research to provide much needed information on in situ burning.

REFERENCES

Aeppli, C., C.A. Carmichael, R.K. Nelson, K.L. Lemkau, W.M. Graham, M.C. Redmond, D.L. Valentine, and C.M. Reddy. 2012. Oil weathering after the Deepwater Horizon disaster led to the formation of oxygenated residues. *Environmental Science & Technology* 46:8,799–8,807, https://doi.org/10.1021/es3015138.

Aeppli, C., C.M. Reddy, R.K. Nelson, M.Y. Kellermann, and D.L. Valentine. 2013. Recurrent oil sheens at the Deepwater Horizon disaster site fingerprinted with synthetic hydrocarbon drilling fluids. *Environmental Science & Technology* 47:8,211–8,219, https://doi.org/10.1021/es4024139.

Aeppli, C., R.K. Nelson, J.R. Radović, C.A. Carmichael, D.L. Valentine, and C.M. Reddy. 2014. Recalcitrance and degradation of petroleum biomarkers in Deepwater Horizon oil upon abiotic and biotic natural weathering. *Environmental Science & Technology* 48:6,726–6,734, https://doi.org/10.1021/es500825q.

Aeppli, C., R.F. Swarthout, G.W. O'Neil, S.D. Katz, D. Nabi, C.P. Ward, R.K. Nelson, C.M. Sharpless, and C.M. Reddy. 2018. How persistent and bioavailable are oxygenated Deepwater Horizon oil transformation products? *Environmental Science & Technology* 52:7,250–7,258, https://doi.org/10.1021/acs.est.8b01001.

Aurell, J., and B.K. Gullett. 2010. Aerostat sampling of PCDD/PCDF emissions from the Gulf oil in situ burns. *Environmental Science & Technology* 44:9,431–9,437, https://doi.org/10.1021/es103554y.

Baelum, J., S. Borglin, R. Chakraborty, J.L. Fortney, R. Lamendella, O.U. Mason, M. Auer, M. Zemla, M. Bill, M.E. Conrad, and others. 2012. Deep-sea bacteria enriched by oil and dispersant from the Deepwater Horizon spill. *Environmental Microbiology* 14:2,405–2,416, https://doi.org/10.1111/j.1462-2920.2012.02780.x.

Booher, L.E., and B. Janke. 1997. Air emissions from petroleum hydrocarbon fires during controlled burning. *American Industrial Hygiene Association Journal* 58:359–365, https://doi.org/10.1080/15428119791012720.

Brocks, J.J., and A. Pearson. 2005. Building the biomarker tree of life. *Reviews in Mineralogy and Geochemistry* 59:233–258, https://doi.org/10.2138/rmg.2005.59.10.

Brocks, J.J., and R.E. Summons. 2014. Sedimentary hydrocarbons, biomarkers for early life. Pp. 61–103 in *Treatise on Geochemistry,* 2nd ed., vol. 10. H. Holland and K. Turekian, eds, Elsevier, Amsterdam, The Netherlands, https://doi.org/10.1016/B978-0-08-095975-7.00803-2.

Bullock, R.J., R.A. Perkins, and S. Aggarwal. 2019. In situ burning with chemical herders for Arctic oil spill response: Meta-analysis and review. *Science of the Total Environment* 675:705–716, https://doi.org/10.1016/j.scitotenv.2019.04.127.

Campo, P., A.D. Venosa, and M.T. Suidan. 2013. Biodegradability of Corexit 9500 and dispersed South Louisiana crude oil at 5 and 25°C. *Environmental Science & Technology* 47:1,960–1,967, https://doi.org/10.1021/es303881h.

Chanton, J., T. Zhao, B.E. Rosenheim, S. Joye, S. Bosman, C. Brunner, K.M. Yeager, A.R. Diercks, and D. Hollander. 2015. Using natural abundance radiocarbon to trace the flux of petrocarbon to the

seafloor following the Deepwater Horizon oil spill. *Environmental Science & Technology* 49:847–854, http://doi.org/10.1021/es5046524.

Daling, P.S., F. Leirvik, I.K. Almås, P.J. Brandvik, B.H. Hansen, A. Lewis, and M. Reed. 2014. Surface weathering and dispersibility of MC252 crude oil. *Marine Pollution Bulletin* 87:300–310, https://doi.org/10.1016/j.marpolbul.2014.07.005.

de Gouw, J.A., A.M. Middlebrook, C. Warneke, R. Ahmadov, E.L. Atlas, R. Bahreini, D.R. Blake, C.A. Brock, J. Brioude, D.W. Fahey, and others. 2011. Organic aerosol formation downwind from the Deepwater Horizon oil spill. *Science* 331:1,295–1,299, https://doi.org/10.1126/science.1200320.

Drozd, G.T., D.R. Worton, C. Aeppli, C.M. Reddy, H. Zhang, E. Variano, and A.H. Goldstein. 2015. Modeling comprehensive chemical composition of weathered oil following a marine spill to predict ozone and potential secondary aerosol formation and constrain transport pathways. *Journal of Geophysical Research* 120:7,300–7,315, https://doi.org/10.1002/2015JC011093.

Evans Seeley, M., Q. Wang, H. Bacosa, B.E. Rosenheim, and Z. Liu. 2018. Environmental petroleum pollution analysis using ramped pyrolysis-gas chromatography–mass spectrometry. *Organic Geochemistry* 124:180–189, https://doi.org/10.1016/j.orggeochem.2018.07.012.

Farrington, J.W., E.B. Overton, and U. Passow. 2021. Biogeochemical processes affecting the fate of discharged Deepwater Horizon gas and oil: New insights and remaining gaps in our understanding. *Oceanography* 34(1):76–97, https://doi.org/10.5670/oceanog.2021.118.

Fritt-Rasmussen, J., and S. Wegeberg. 2015. Review on burn residues from in situ burning of oil spills in relation to Arctic waters. *Water, Air, and Soil Pollution* 226:329, https://doi.org/10.1007/s11270-015-2593-1.

Gaines, R.B., G.S. Frysinger, M.S. Hendrick-Smith, and J.D. Stuart. 1999. Oil spill source identification by comprehensive two-dimensional gas chromatography. *Environmental Science & Technology* 33:2,106–2,112, https://doi.org/10.1021/es9810484.

Gaines, S.M., G.E. Eglinton, and J. Rullkötter. 2009. *Echoes of Life: What Fossil Molecules Reveal about Earth History*. Oxford University Press, New York, NY, 357 pp.

Gros, J., C.M. Reddy, C. Aeppli, R.K. Nelson, C.A. Carmichael, and J.S. Arey. 2014. Resolving biodegradation patterns of persistent saturated hydrocarbons in weathered oil samples from the Deepwater Horizon disaster. *Environmental Science & Technology* 48:1,628–1,637, https://doi.org/10.1021/es4042836.

Gros, J., C.M. Reddy, R.K. Nelson, S.A. Socolofsky, and J.S. Arey. 2016. Simulating gas-liquid-water partitioning and fluid properties of petroleum under pressure: Implications for deep-sea blowouts. *Environmental Science & Technology* 50:7,397–7,408, https://doi.org/10.1021/acs.est.5b04617.

Gros, J., S.A. Socolofsky, A.L. Dissanayake, I. Jun, L. Zhao, M.C. Boufadel, C.M. Reddy, and J.S. Arey. 2017. Petroleum dynamics in the sea and influence of subsea dispersant injection during Deepwater Horizon. *Proceedings of the National Academy of Sciences of the United States of America* 114:10,065–10,070, https://doi.org/10.1073/pnas.1612518114.

Gullett, B.K., M.D. Hayes, D. Tabor, and R. Vander Wal. 2016. Characterization of the particulate emissions from the BP Deepwater Horizon surface oil burns. *Marine Pollution Bulletin* 107:216–223, https://doi.org/10.1016/j.marpolbul.2016.03.069.

Gullett, B.K., J. Aurell, A. Holder, W. Mitchell, D. Greenwell, M. Hays, R. Conmy, D. Tabor, W. Preston, I. George, and others. 2017. Characterization of emissions and residues from simulations of the Deepwater Horizon surface oil burns. *Marine Pollution Bulletin* 117:392–405, https://doi.org/10.1016/j.marpolbul.2017.01.083.

Halanych, K.M., C.H. Ainsworth, E.E. Cordes, R.E. Dodge, M. Huettel, I.A. Mendelssohn, S.A. Murawski, C.B. Paris-Limouzy, P.T. Schwing, R.F. Shaw, and T. Sutton. 2021. Effects of petroleum by-products and dispersants on ecosystems. *Oceanography* 34(1):152–163, https://doi.org/10.5670/oceanog.2021.123.

Hall, G.J., G.S. Frysinger, C. Aeppli, C.A. Carmichael, J. Gros, K.L. Lemkau, R.K. Nelson, and C.M. Reddy. 2013. Oxygenated weathering products of Deepwater Horizon oil come from surprising precursors. *Marine Pollution Bulletin* 75:140–149, https://doi.org/10.1016/j.marpolbul.2013.07.048.

He, M., J.M. Moldowan, and K.E. Peters. 2018. Biomarkers: Petroleum. Pp. 1–13 in *Encyclopedia of Geochemistry, Living Edition*. W.M. White, ed., Springer International Publishing AG, Basel, Switzerland, https://doi.org/10.1007/978-3-319-39193-9_170-1.

Hunt, J.M. 1996. *Petroleum Geochemistry and Geology*, 2nd ed. W.H. Freeman and Company, New York, 743 pp.

Isaacs, C.M. 2001. Statistical evaluation of interlaboratory data from the Cooperative Monterey Organic Geochemistry Study. Pp. 461–524 in *The Monterey Formation: From Rocks to Molecules*. C.M. Isaacs and J. Rullkötter, eds, Columbia University Press, New York.

Jaggi, A., J.R. Radović, L.R. Snowdon, S.R. Larter, and T.B.P. Oldenburg. 2019. Composition of the dissolved organic matter produced during in situ burning of spilled oil. *Organic Geochemistry* 138:103926, https://doi.org/10.1016/j.orggeochem.2019.103926.

Jarvie, D.M, B.M. Jarvie, D. Weldon, and A. Maende. 2015. Geochemical assessment of in situ petroleum in unconventional resource systems. *Proceedings of the 3rd Unconventional Resources Technology Conference 201*5, http://fianum.com/files/articles/1/GeochemicaAssessment.pdf.

Johansson, K.O., M.P. Head-Gordon, P.E. Schrader, K.R. Wilson, and H.A. Michelsen. 2018. Resonance-stabilized hydrocarbon-radical chain reactions may explain soot inception and growth. *Science* 381:997–1,000, https://doi.org/10.1126/science.aat3417.

Kessler, J.D., D.L. Valentine, M.C. Redmond, M. Du, E.W. Chan, S.D. Mendes, E.W. Quiroz, C.J. Villanueva, S.S. Shusta, L.M. Werra, and others. 2011. A persistent oxygen anomaly reveals the fate of spilled methane in the deep Gulf of Mexico. *Science* 331:312–315, http://doi.org/10.1126/science.1199697.

Kujawinski, E.B., M.C. Kido Soule, D.L. Valentine, A.K. Boysen, K. Longnecker, and M.C. Redmond. 2011. Fate of dispersants associated with the Deepwater Horizon oil spill. *Environmental Science & Technology* 45:1,298–1,306, https://doi.org/10.1021/es103838p.

Kujawinski, E.B., C.M. Reddy, R.P. Rodgers, J.C. Thrash, D.L. Valentine, and H.K. White. 2020. The first decade of scientific insights from the Deepwater Horizon oil release. 2020. *Nature Reviews Earth & Environment* 1:237–250, https://doi.org/10.1038/s43017-020-0046-x.

Lee, Y.G, X. Garza, and R.M. Lee. 2018. Ultimate costs of the disaster: Seven years after the Deepwater Horizon oil spill. *Journal of Corporate Accounting & Finance* 29:69–79, https://doi.org/10.1002/jcaf.22306.

Lehr, B., S. Bristol, and A. Possolo. 2010. *Oil Budget Calculator Deepwater Horizon. Technical Documentation, A Report to the National Incident Command*, *November 2010*. http://www.restorethegulf.gov/sites/default/files/documents/pdf/OilBudgetCalc_Full_HQ-Print_111110.pdf.

Lima, A.L.C., J.W. Farrington, and C.M. Reddy. 2005. Combustion-derived polycyclic aromatic hydrocarbons in the environment: A review. *Environmental Forensics* 6:109–131, https://doi.org/10.1080/15275920590952739.

Litman, E., S. Emsbo-Mattingly, and W. Wong. 2018. Critical review of an interlaboratory forensic dataset: Effects on data interpretation in oil spill studies. Pp. 1–23 in *Oil Spill Environmental Forensics Case Studies*. S.A. Stout, and Z. Wang, eds, Butterworth-Heinemann, Elsevier, Oxford, UK, https://doi.org/10.1016/B978-0-12-804434-6.00001-X.

MacDonald, I.R., O. Garcia-Pineda, A. Beet, S. Daneshgar Asl, L. Feng, G. Graettinger, D. French-McCay, J. Holmes, C. Hu, F. Huffer, and others. 2015. Natural and unnatural oil slicks in the Gulf of Mexico. *Journal of Geophysical Research* 120:8,364–8,380, https://doi.org/10.1002/2015JC011062.

Mackenzie, A.S. 1984. Application of biological markers in petroleum geochemistry. Pp. 115–214 in *Advances in Petroleum Geochemistry,* vol. 1. J. Brooks and D.H. Welte, eds, Academic Press, London, UK.

McKenna, A.M., R.K. Nelson, C.M. Reddy, J.J. Savory, N.K. Kaiser, J.E. Fitzsimmons, A.G. Marshall, and R.P. Rodgers. 2013. Expansion of the analytical window for oil spill characterization by ultra-high resolution mass spectrometry: Beyond gas chromatography. *Environmental Science & Technology* 47:7,530–7,539, https://doi.org/10.1021/es305284t.

Mello, M.R., N. Telnæs, P.C. Gaglianone, M.I. Chicarelli, S.C. Brassell, and J.R. Maxwell. 1988. Organic geochemical characterisation of depositional palaeoenvironments of source rocks and oils in Brazilian marginal basins. *Organic Geochemistry* 13:31–45, https://doi.org/10.1016/0146-6380(88)90023-X.

Murawski, S.A., M. Grosell, C. Smith, T. Sutton, K.M. Halanych, R.F. Shaw, and C.A. Wilson. 2021. Impacts of petroleum, petroleum components, and dispersants on organisms and populations. *Oceanography* 34(1):136–151, https://doi.org/10.5670/oceanog.2021.122.

Murray, J.A., L.C. Sander, S.A. Wise, and C.M Reddy. 2016. Gulf of Mexico Research Initiative 2014–2015 Hydrocarbon Intercalibration Experiment: Description of results for SRM 2779 Gulf of Mexico crude oil and Candidate SRM 2777 weathered Gulf of Mexico crude oil. *NIST Interagency/Internal Report 8123*, created April 20, 2016, updated November 10, 2018, https://doi.org/10.6028/NIST.IR.8123.

Niles, S.F., M.L. Chacón-Patiño, H. Chen, A.M. McKenna, G.T. Blakney, R.P. Rodgers, and A.G. Marshall. 2019. Molecular-level characterization of oil-soluble ketone/aldehyde photo-oxidation products by Fourier transform ion cyclotron resonance mass spectrometry reveals similarity between microcosm and field samples. *Environmental Science & Technology* 53:6,887–6,894, https://doi.org/10.1021/acs.est.9b00908.

NIST (National Institute of Standards and Technology). 2020. Technical details of SRM 2779, Gulf of Mexico crude oil, https://www-s.nist.gov/srmors/view_detail.cfm?srm=2779.

Nixon, Z., S. Zengel, M. Baker, M. Steinhoff, G. Fricano, S. Rouhani, and J. Michel. 2016. Shoreline oiling from the Deepwater Horizon oil spill. *Marine Pollution Bulletin* 107:170–178, https://doi.org/10.1016/j.marpolbul.2016.04.003.

NOAA Office of Response and Restoration. 2020. Residues from in situ burning of oil on water, https://response.restoration.noaa.gov/oil-and-chemical-spills/oil-spills/resources/residues-in-situ-burning-oil-water.html.

Oldenburg, T.B.P., M. Brown, B. Bennett, and S.R. Larter. 2014. The impact of thermal maturity level on the composition of crude oils, assessed using ultra-high resolution mass spectrometry. *Organic Geochemistry* 75:151–168, https://doi.org/10.1016/j.orggeochem.2014.07.002.

Oldenburg, T.B.P., P. Jaeger, J. Gros, S.A. Socolofsky, S. Pesch, J.R. Radović, and A. Jaggi. 2020. Physical and chemical properties of oil and gas under reservoir and deep-sea conditions. Pp. 25–42 in *Deep Oil Spills*. S.A. Murawski, C.H. Ainsworth, S. Gilbert, D.J. Hollander, C.B. Paris, M. Schlüter, and D.L. Wetzel, eds, Springer Nature Switzerland, Cham, Switzerland, https://doi.org/10.1007/978-3-030-11605-7_3.

Overton, E.B., T.L. Wade, J.R. Radović, B.M. Meyer, M.S. Miles, and S.R. Larter. 2016. Chemical composition of Macondo and other crude oils and compositional alterations during oil spills. *Oceanography* 29:50–63, https://doi.org/10.5670/oceanog.2016.62.

Passow, U., and S.A. Stout. 2020. Character and sedimentation of "lingering" Macondo oil to the deep-sea after the Deepwater Horizon oil spill. *Marine Chemistry* 218:103733, https://doi.org/10.1016/j.marchem.2019.103733.

Perring, A.E., J.P. Schwarz, J.R. Spackman, R. Bahreini, J.A. de Gouw, R.S. Gao, J.S. Holloway, D.A. Jack, J.M. Langridge, J. Peischl, and others. 2011. Characteristics of black carbon aerosol from a surface oil burn during the Deepwater Horizon oil spill. *Geophysical Research Letters* 38(17), https://doi.org/10.1029/2011GL048356.

Peters, K.E., C.C. Walters, and J.M. Moldowan. 2005a. *The Biomarker Guide: Volume 1, Biomarkers and Isotopes in the Environment and Human History*. Columbia University Press, New York, NY, 481 pp.

Peters, K.E., C.C. Walters, and J.M. Moldowan. 2005b. *The Biomarker Guide: Volume 2, Biomarkers and Isotopes in Petroleum Exploration and Earth History*. Columbia University Press, New York, NY, 704 pp.

Quigg, A., J.W. Farrington, S. Gilbert, S.A. Murawski, and V.T. John. 2021. A decade of GoMRI dispersant science: Lessons learned and recommendations for the future. *Oceanography* 34(1):98–111, https://doi.org/10.5670/oceanog.2021.119.

Radke, M., and D.H. Welte. 1983. The Methylphenanthrene Index (MPI): A maturity parameter based on aromatic hydrocarbons. Pp. 504–512 in *Advances in Organic Geochemistry, 1981: Proceedings of the 10th International Meeting on Organic Geochemistry. University of Bergen, Norway, 14–18 September 1981*. M. Bjorøy, ed., Wiley & Sons, Chichester, UK.

Radke, M., H. Willsch, and D.H. Welte. 1984. Class separation of aromatic compounds in rock extracts and fossil fuels by liquid chromatography. *Analytical Chemistry* 56:2,538–2,546, https://doi.org/10.1021/ac00277a061.

Reddy, C.M., J.S. Arey, J.S. Seewald, S.P. Sylva, K.L. Lemkau, R.K. Nelson, C.A. Carmichael, C.P. McIntyre, J. Fenwick, G.T. Ventura, and others. 2012. Composition and fate of gas and oil released to the water column during the Deepwater Horizon oil spill. *Proceedings of the National Academy of Sciences of the United States of America* 109:20,229–20,234, https://doi.org/10.1073/pnas.1101242108.

Rossini, F.D., and B.J. Mair. 1959. The work of the API research project 6 on the composition of petroleum. Pp. 223–245 in *Proceeding of the 5th World Petroleum Congress*, Sec. V, Paper 18.

Ruddy, B.M., M. Huettel, J.E. Kostka, V.V. Lobodin, B.J. Bythell, A.M. McKenna, C. Aeppli, C.M. Reddy, R.K. Nelson, A.G. Marshall, and R.P. Rodgers. 2014. Targeted petroleomics: Analytical investigation of Macondo well oil oxidation products from Pensacola Beach. *Energy & Fuels* 28:4,043–4,050, https://doi.org/10.1021/ef500427n.

Rullkötter, J., and W. Michaelis. 1990. The structure of kerogen and related materials: A review of recent progress and future trends. *Organic Geochemistry* 16:829–852, https://doi.org/10.1016/0146-6380(90)90121-F.

Ryerson, T.B., K.C. Aikin, W.M. Angevine, E.L. Atlas, D.R. Blake, C.A. Brock, F.C. Fehsenfeld, R.-S. Gao, J.A. de Gouw, D.W. Fahey, and others. 2011. Atmospheric emissions from the Deepwater Horizon spill constrain air-water partitioning, hydrocarbon fate, and leak rate. *Geophysical Research Letters* 38(7), https://doi.org/10.1029/2011GL046726.

Ryerson, T.B., R. Camilli, J.D. Kessler, E.B. Kujawinski, C.M. Reddy, D.L. Valentine, E. Atlas, D.R. Blake, J. de Gouw, S. Meinardi, and others. 2012. Chemical data quantify Deepwater Horizon hydrocarbon flow rate and environmental distribution. *Proceedings of the National Academy of Sciences of the United States of America* 109:20,246–20,253, https://doi.org/10.1073/pnas.1110564109.

Sandifer, P.A., A. Ferguson, M.L. Finucane, M. Partyka, H.M. Solo-Gabriele, A.H. Walker, K. Wowk, R. Caffey, and D. Yoskowitz. 2021. Human health and socioeconomic effects of the Deepwater Horizon oil spill in the Gulf of Mexico. *Oceanography* 34(1):174–191, https://doi.org/10.5670/oceanog.2021.125.

Schaum, J., M. Cohen, S. Perry, R. Artz, R. Draxler, J.B. Frithsen, D. Heist, M. Lorber, and L. Phillips. 2010. Screening level assessment of risks due to dioxin emissions from burning oil from the BP Deepwater Horizon Gulf of Mexico spill. *Environmental Science & Technology* 44:9,383–9,389, https://doi.org/10.1021/es103559w.

Seifert, W.K., and J.M. Moldowan. 1986. Use of biological markers in petroleum exploration. Pp. 261–290 in *Methods in Geochemistry and Geophysics, Volume 24*. R.B. Johns, ed., Elsevier, Amsterdam, The Netherlands.

Sherwood Lollar, B., T.D. Westgate, J.A. Ward, G.F. Slater, and G. Lacrampe-Couloume. 2002. Abiogenic formation of alkanes in the Earth's crust as a minor source for global hydrocarbon reservoirs. *Nature* 416:522–524, https://doi.org/10.1038/416522a.

Smith, H.M. 1968. *Qualitative and Quantitative Aspects of Crude Oil Composition*. United States Bureau of Mines Bulletin 642, United States Department of the Interior, Washington, DC, 136 pp.

Snowdon, L.R., J.K. Volkman, Z. Zhang, G. Tao, and P. Liu. 2016. The organic geochemistry of asphaltenes and occluded biomarkers. *Organic Geochemistry* 91:3–15, https://doi.org/10.1016/j.orggeochem.2015.11.005.

Speight, J.G. 2015. *Handbook of Petroleum Product Analysis*, 2nd ed. Wiley-Interscience, Hoboken, 351 pp.

Stout, S.A., and J.R. Payne. 2016. Chemical composition of floating and sunken in situ burn residues from the Deepwater Horizon oil spill. *Marine Pollution Bulletin* 108:186–202, https://doi.org/10.1016/j.marpolbul.2016.04.031.

Stout, S.A., and Z. Wang, eds. 2018. *Oil Spill Environmental Forensics Case Studies*. Butterworth-Heinemann, Elsevier, Oxford, UK, 860 pp, https://doi.org/10.1016/B978-0-12-804434-6.00035-5.

Summons R.E., L.L. Jahnke, J.M. Hope, and G.A. Logan. 1999. 2-methylhopanoids as biomarkers for cyanobacterial oxygenic photosynthesis. *Nature* 400:554–557, https://doi.org/10.1038/23005.

Tawfiq, N., and D. Olsen. 1993. Saudi Arabia's response to the 1991 Gulf oil spill. *Marine Pollution Bulletin* 27:333–345, https://doi.org/10.1016/0025-326X(93)90041-H.

Tissot, B.P, and D.H. Welte. 1984. *Petroleum Formation and Occurrence*, 2nd ed. Springer, Heidelberg, 699 pp.

Valentine, D.L., J.D. Kessler, M.C. Redmond, S.D. Mendes, M.B. Heintz, C. Farwell, L. Hu, F.S. Kinnaman, S. Yvon-Lewis, M. Du, and others. 2010. Propane respiration jump-starts microbial response to a deep oil spill. *Science* 330:208–211, http://doi.org/10.1126/science.1196830.

Van den Berg, M., L.S. Birnbaum, M. Dennison, M. De Vito, W. Farland, M. Feeley, H. Fiedler, H. Hakansson, A. Hanberg, L. Haws, and others. 2006. The 2005 World Health Organization re-evaluation of human and mammalian toxic equivalency factors for dioxins and dioxin-like compounds. *Toxicological Science* 93:223–241, https://doi.org/10.1093/toxsci/kfl055.

Vitha, M.F. 2016. *Chromatography: Principles and Instrumentation.* Wiley & Sons, Hoboken, NJ, 268 pp.

Wang, Q., B. Leonce, M.E. Seeley, N.F. Adegboyega, K. Lu, W.C. Hockaday, and Z. Liu. 2020. Elucidating the formation pathway of photo-generated asphaltenes from light Louisiana sweet crude oil after exposure to natural sunlight in the Gulf of Mexico. *Organic Geochemistry* 150:104126, https://doi.org/10.1016/j.orggeochem.2020.104126.

Welte, D.H., B. Horsfield, and D.R. Baker, eds. 1997. *Petroleum and Basin Evolution*. Springer, Berlin, Heidelberg, 535 pp.

White, H.K., R.N. Conmy, I.R. MacDonald, and C.R. Reddy. 2016a. Methods of oil detection in response to the Deepwater Horizon oil spill. *Oceanography* 29:76–87, https://doi.org/10.5670/oceanog.2016.72.

White, H.K., C.H. Wang, P.L. Williams, D.M. Findley, A.M. Thurston, R.L. Simister, C. Aeppli, R.K. Nelson, and C.M. Reddy. 2016b. Long-term weathering and continued oxidation of oil residues from the Deepwater Horizon spill. *Marine Pollution Bulletin* 113:380–386, https://doi.org/10.1016/j.marpolbul.2016.10.029.

Yang, C., G. Zhang, Z. Wang, Z. Yang, B. Hollebone, M. Landriault, K. Shah, and C.E. Brown. 2014. Development of a methodology for accurate quantitation of alkylated polycyclic aromatic hydrocarbons in petroleum and oil contaminated environmental samples. *Analytical Methods* 6:7,760–7,771, https://doi.org/10.1039/C4AY01393J.

Zito, P., D.C. Podgorski, T. Bartges, F. Guillemette, J.A. Roebuck Jr., R.G.M. Spencer, R.P. Rodgers, and M.A. Tarr. 2020. Sunlight-induced molecular progression of oil into oxidized oil soluble species, interfacial material, and dissolved organic matter. *Energy & Fuels* 34(4):4,721–4,726, https://doi.org/10.1021/acs.energyfuels.9b04408.

ACKNOWLEDGMENTS

Brian Gullett (US Environmental Protection Agency), Elisabeth Kujawinski (Woods Hole Oceanographic Institution), Thomas Oldenburg (University of Calgary, Canada), and Ryan Rodgers (National High Magnetic Field Laboratory) were kind enough to review an early version of the manuscript. We are indebted to Kenneth E. Peters (Schlumberger) and Roger E. Summons (Earth, Atmospheric, and Planetary Sciences, MIT) for carefully reviewing the final manuscript and providing helpful scientific comments and technical edits for improvement. We also thank the GoMRI Management Team for their support in the preparation and submission of the manuscript.

AUTHORS

Jürgen Rullkötter (juergen.rullkoetter@uni-oldenburg.de) is Professor (retired), Institute of Chemistry and Biology of the Marine Environment, Carl von Ossietzky University of Oldenburg, Oldenburg, Germany. **John W. Farrington** is Dean Emeritus, Marine Chemistry and Geochemistry Department, Woods Hole Oceanographic Institution, Woods Hole, MA, USA.

ARTICLE CITATION

Rullkötter, J., and J.W. Farrington. 2021. What was released? Assessing the physical properties and chemical composition of petroleum and products of burned oil. *Oceanography* 34(1):44–57, https://doi.org/10.5670/oceanog.2021.116.

COPYRIGHT & USAGE